ChemComm

Accepted Manuscript

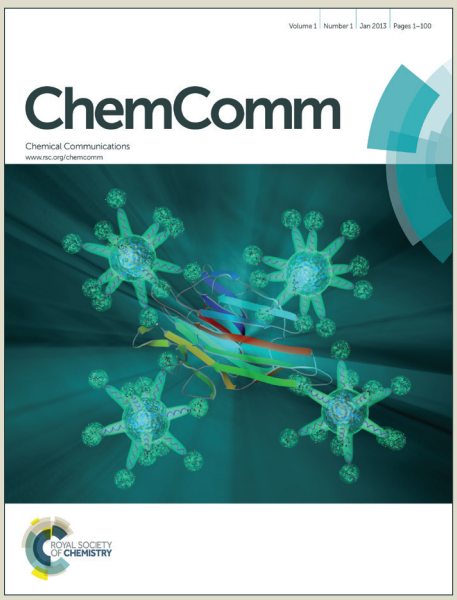

ROYAL SOCIETY OF CHEMISTRY

www.rsc.org/chemcomm

Cite this: DOI: 10.1039/c0xx00000x

www.rsc.org/xxxxxx

ARTICLE TYPE

p-Benzoquinone adsorption/separation, sensing and its photoinduced transformation within a robust Cd(II)-MOF in a SC-SC fashion

Fan Yang, Qi-Kui Liu,* Dan Wu, An-Yan Li, and Yu-Bin Dong*

Received (in XXX, XXX) Xth XXXXXXXXX 20XX, Accepted Xth XXXXXXXXX 20XX

DOI: 10.1039/b000000x

***p*-Benzoquinone (Q) adsorption/separation, sensing and its photoinduced transformation within a robust Cd(II)-MOF (1) is reported. All the adsorption, sensing and photochemical reactions are directly performed on the single-crystals of 1.**

Because of their numerous potential applications, metal-organic frameworks (MOFs) are of considerable interest in chemistry and materials science.[1] One of the most promising applications for MOFs might be their use as porous materials for molecular adsorption, separation and sensing.[2] As a host, the porous MOF can sometimes accommodate two or more substrates which provides an unique opportunity for us to explore the highly controlled chemical reactions of the encapsulated species within the inner space. It is now clear that the molecular behavior within a confined space in the solid state is somehow different from that in solution.[3]

On the other hand, single MOF-crystals have been shown to tolerate considerable dynamic behavior at the molecular level while maintaining their single-crystal character.[4] Compared to the bulk samples, the investigation based on discrete MOF-single crystals is relatively rare. The study on single-crystallinity-maintained MOFs would provide the more direct evidence at molecular-level for gaining better understanding the phenomena of guest uptake, realease, or exchange as well as chemical transformations in the solid state.

p-Benzoquinone (**Q**), as a fully conjugated cyclic dione, is widely used as a chemical intermediate, a polymerization inhibitor, an oxidizing agent, a photographic chemical and a tanning agent.[5] On the other hand, acute exposure to high levels of **Q**, via inhalation in humans, is highly irritating to the eyes, resulting in discoloration of the conjunctiva and cornea, while dermal exposure causes dermatitis with skin discoloration and erythema.[6] In addition, **Q** is confirmed to be the main intermediate of *p*-hydroquinone (**QH_2**) degradation.[7] Moreover, **Q** is even much more toxic than **QH_2**.[8] So the **Q** sensing, and the separation of **Q** from **QH_2** are very important.

In this contribution, we report **Q** adsorption, sensing, photoinduced transformation and **Q/QH_2** separation based on a porous Cd(II)-MOF. The Cd(II)-MOF crystals are robust and can keep their macroscopic integrity during the processes.

The adsorption of **Q** was performed on a porous 3D MOF $H_2O{\subset}Cd(L)_2(ClO_4)_2$ (**1**, L = 4-amino-3,5-bis(4-pyridyl-3-phenyl)-1,2,4-triazole), which was previously reported by us.[9] It contains square-like channels (dimensions ~11 × 11 Å). For a practical purpose, the Q adsorption was carried out in an aqueous media. When the crystals of **1** were immersed in an aqueous solution of **Q** (55 mg/L, glucose degradation by an Escherichia coli is inhibited at this concentration) at ambient temperature for 72 h, the colorless crystals of **1** changed to light brown with retention of their single-crystal nature (Figure 1). Single-crystal X-ray diffraction revealed that the **Q** guests are located in the pores of **1** to generate a new host-guest system of **$Q{\subset}[CdL_2{\cdot}(ClO_4)_2]$** (**2**) (‡). The uploaded **Q** was further confirmed by the thermogravimetric analysis (TGA) (Figure S1, ESI†). As shown in Figure 2a, the encapsulated **Q** is held in place

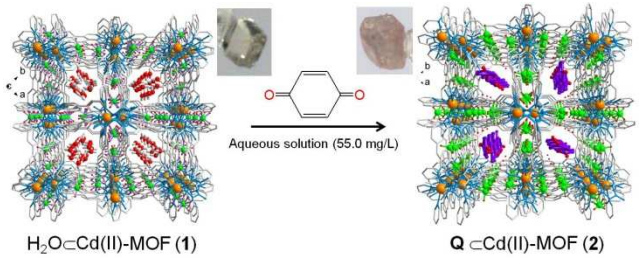

Figure 1. Q adsorption based on **1** in a SC-SC fashion (single-crystal X-ray diffraction indicates that the loaded Q species are disordered in the pores, so only the major disordered components are shown). The single crystal photographs of **1** and **2** are inserted.

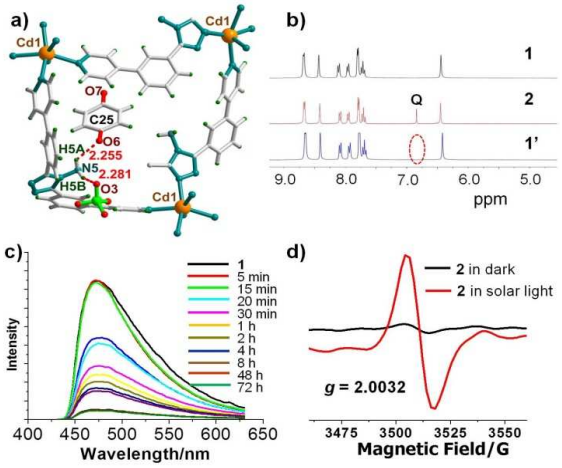

Figure 2. a) Host-guest H-bonding system found in **2**; b) ^{1}H NMR spectra (300 MHz, DMSO-d_6) of **1**, **2** and regenerated **1** (**1'**); c) the solid state emission spectra of **1** (λ_{ex} = 328 nm) recorded during the **Q** adsorption process; d) the ESR spectra of **2** in dark and in simulated solar light.

via N-H···O bond ($d_{O\cdots H}$ = 2.255 Å, $d_{O\cdots N}$ = 2.848 Å and <N-H···O = 123°) which is consisting of the -NH_2 group from the framework and the one terminal O atom of **Q**. Compared to **1**, the new proton resonance at 6.86 ppm in the ^{1}H NMR spectrum further supports the uptake of **Q** in **2** (Figure 2b). On the other hand, the uploaded **Q** can be further removed by extracting (by MeOH and CH_3CN) to regenerate the **Q**-free framework of **1** (**1'**) (Figure 2b). Besides single-crystal X-ray diffraction, the X-ray powder diffraction (XRPD) patterns of **1**, **2** and **1'** are identical, suggesting that the framework of the Cd(II)-MOF keeps no change on the bulk samples upon this reversible guest adsorption. (Figure S2, ESI†). So the Cd(II)-MOF is reusable.

Cd(II)-MOF (**1**), as a fluorescent sensor for detecting **Q**, was fortuitously found by the solid-state luminescence monitoring. As shown in Figure 2c, **1** exhibits strong emission at ca. 450 nm upon excitation at 328 nm, corresponding to a distinct blue color. After **Q** loading, the emission of **1**, however, is strongly quenched. Figure 2c shows that the emission intensity of **1** decreased by degrees as time progressed. The emission of **1** was almost completely quenched in ca. 48h. It is known that **Q**, as an H-bond acceptor, can associate with H-bond donor via H-bonding interaction to generate the nonfluorescent supramolecular adduct in solution, which is resulted from an efficient intracomplex photoinduced electron transfer in close vicinity.[10] It is distinctly different from that in solution, the luminescence quenching herein is resulted from the formation of radical species instead of nonfluorescent CdL_2-**Q** adduct in the solid state. As shown in Figure 2d, the steady-state electron spin resonance (ESR) spectrum of **2** shows no signal in dark, but the signal appeared upon exposure to solar light. The obtained *g* value (2.0032) confirms the formation of **Q** radical.[11] So the luminescence quenching is clearly caused by the formation of radical species within the CdL_2 framework. The constrictive encapsulation within a confined space might facilitate the proton-coupled electron transfer to generate photoinduced **Q** radical assisted by the H-bonding interactions (no ESR signal observed on the free solid benzoquinone irridiated by simulated solar light, Figure S3, ESI†).[12] Notably, the **Q** radical is alive for a considerable long time within the pores in air under ambient conditions.

As a useful sensor, effective detection of the target species at a low concentration is important. The permitted concentrations of Q in the discharged wastewater and water body are 1.0 and 0.2 mg/L (USSR, 1975) respectively. So the **Q** adsorption based on **1** was carried out in 1.0 and 0.2 mg/L aqueous solutions.

Similarly, the emission of **1** could also be strongly quenched when Cd(II)-MOF suspended in the more dilute **Q** aqueous solutions (1.0 and 0.2 mg/L). Figure 3 shows that the emission intensity was visibly quenched after 1 h (1.0 mg/L) and 4 h (0.2 mg/L), and the weakest emission was observed at 96 h (1.0 mg/L) and 120 h (0.2 mg/L), respectively. In addition, the sensitivity of **1** was also evaluated in a **Q** aqueous solution at 0.02 mg/L, we found it can effectively detect **Q** at this concentration (Figure S4, ESI†). Again, the Cd(II)-MOF framework is intact during these guest uptake processes (Figure 3).

The photochemistry of **Q** has attracted considerable attention for decades.[13] In the solid state, **Q** is photoinert. However, **Q** can be photolyzed in some H-donor media such as water and alcohol, and they all go through with a radical process.[13] The

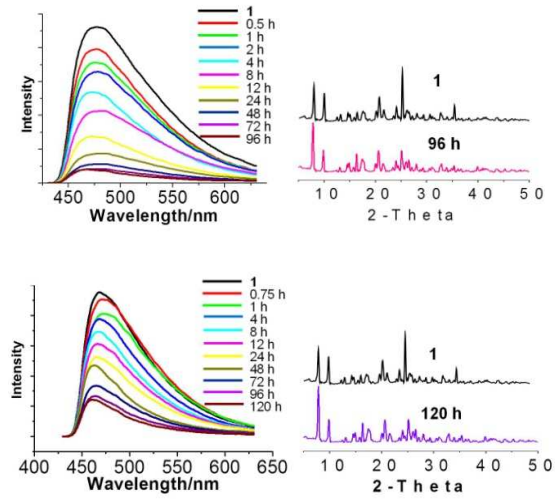

Figure 3. Top: the solid state emission spectra of **1** recorded in an aqueous solution of **Q** (1.0 mg/L) and corresponding XRPD patterns; bottom: the solid state emission spectra of **1** recorded in an aqueous solution of **Q** (0.2 mg/L) and corresponding XRPD patterns.

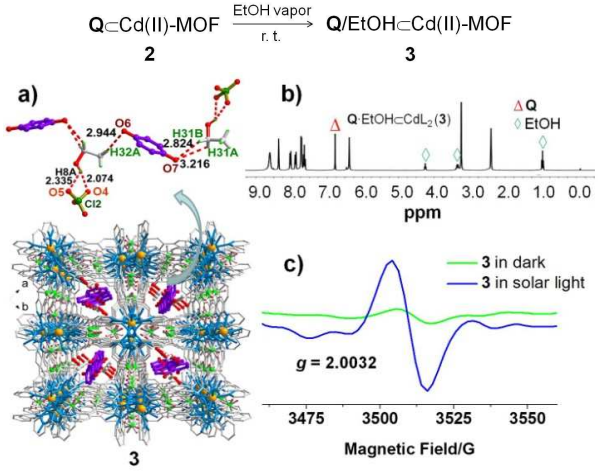

Figure 4. Scheme representation of **2** to **3**. a) Single crystal structure (single-crystal X-ray diffraction indicates that the loaded Q and EtOH species are disordered in the pores, so only the major disordered components are shown) and H-bonding **Q**···EtOH···ClO_4^- system; b) ^{1}H NMR spectrum (300 MHz, DMSO-d_6) of **3**; c) the ESR spectra of **3** in dark and in ambient light.

photochemical study of **Q** within MOF-flask in the solid state is unprecedented. As mentioned above, **Q** exists in the pores as solar light-irradiated radical species which is an active precursor for photochemical reaction. However, when **Q⊂[CdL_2·$(ClO_4)_2$]** (**2**) was exposed to simulated solar light, no photoinduced reaction occurred, indicating that the reaction could not be proceeded in the absence of H-donors.[13] Compound **2** therefore was exposed to EtOH vapor at room temperature. After 2 days, EtOH, as a H-donor substrate, was taken inside to generated **Q·EtOH⊂[CdL_2·$(ClO_4)_2$]** (**3**) (‡). Single-crystal X-ray diffraction revealed that both Q and EtOH are located in the pores of **3**. As shown in Figure 4a, the encapsulated EtOH and **Q** are alternately arranged in the pores and linked together via intermolecular H-bonds into an EtOH···**Q** zigzag chain, to which the ClO_4^- anions are attached through H···O_4Cl^- bonds. Along with the single-crystal X-ray diffraction, different guest species

incorporation into the CdL_2 host was further evidenced by the ^{1}H NMR spectrum (Figure 4b) and TGA (Figure S5, ESI†). XRPD pattern indicates that the bulk sample of **3** is stable (Figure S6, ESI†). It is similar to **2**, compound **3** shows a clear ESR signal corresponding to the **Q** radical species in solar light (Figure 4c).

Compared to **2**, the difference of **3** lies in that the crystal color changed from light brown to pink when the crystals of **3** were exposed to simulated solar light for 24 h (Figure 5). Single-crystal X-ray diffraction indicated that ca. 50 % of **Q** transformed into $\mathbf{QH_2}$ to generate **Q/QH$_2$⊂Cd(II)-MOF** (**4**) (‡), which is well agreement with the ^{1}H NMR spectrum (Figure 5). Notably, if **3** exposed to simulated solar light over 24 h, no more conversion of **Q** could be realized based on ^{1}H NMR spectra (Figure S7, ESI†). The XDPD pattern demonstrated that the Cd(II)-framework is stable (Figure 5).

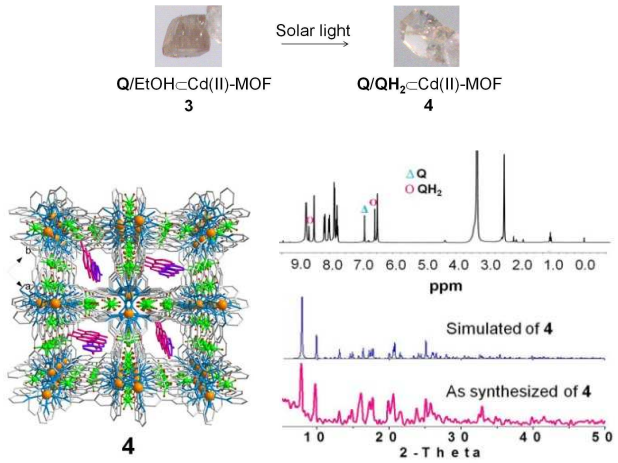

Figure 5. Scheme representation of **3** to **4**, and the corresponding crystal pictures are inserted. Single crystal structure (single-crystal X-ray diffraction indicates that the loaded **Q** (purple) and $\mathbf{QH_2}$ (red) species are disordered in the pores, so only the major disordered components are shown), ^{1}H NMR spectrum (300 MHz, DMSO-d_6), and XRPD patterns of **4**. EtOH (δ = 1.06, 3.45, 4.64 ppm) and CH_3CHO (δ = 2.25, 9.38 ppm) and tiny amount of hydroquinone monoacetate are also found in the ^{1}H NMR spectrum. The simulated and measured XRPD patterns indicate that the Cd(II)-MOF is stable during the photochemical reaction.

Besides single-crystal X-ray diffraction and ^{1}H NMR measurement, the photolysis products were also analyzed by the GC-MS. The result indicated that the reaction generated $\mathbf{QH_2}$, acetaldehyde along with a tiny amount of hydroquinone monoacetate (Figure S8, ESI†). The conversion rate of **Q** in **4** is 65.3 % based on GC analysis.

Notably, the conversion of **Q** herein is closely related to the encapsulated amount of EtOH. More amount of encapsulated EtOH would facilitate the photolysis of **Q** under the reaction conditions. For example, when the ratios of **Q**/EtOH are 1/0.56, 1/1.20, 1/2.77, 1/5.25, 1/8.67 (based on ^{1}H NMR spectra, Figure S9, ESI†), the conversions of **Q** are 34.2, 61.0, 66.3, 77.5 and 77.7%, respectively (Figure 6).

As shown above, the photolysis of **Q** can be smoothly carried out by successive uptake of **Q** and EtOH under simulated solar light. Although we say forthright that we currently cannot describe this photochemical reaction mechanism in detail, the photochemical behavior of **Q** within the Cd(II)-MOF flask is indeed different from that in solution. In solution, **Q** is irradiated

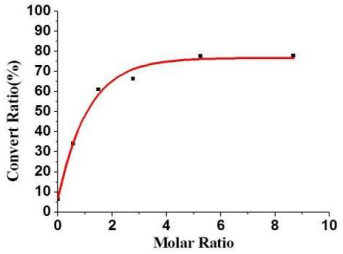

Figure 6. Plot showing the conversion rate of **Q** vs **Q**/EtOH molar ratio in **4**.

by UV light to give rise to its triplet $\mathbf{Q}^{\bullet}$ which is typically described as a photoactive species.[13] By contrast, **Q** within the CdL_2 framework can be irradiated by sunlight to generate more active radical species. So the photoreaction condition is milder. Secondly, the orientations of the substrates are restricted by H-bonding interactions within the confined space, which would facilitate the H-abstraction step.[13] In addition, the photolysis of **Q** within MOF flask is clean. The photolysis of **Q** in EtOH, however, is complicated and produced $\mathbf{QH_2}$, acetaldehyde, 1,1-diethoxyethane, 2-acetylhydroquinone and quinhydrone based on the GC-MS measurement (Figure S10, ESI†). Such difference is clearly resulted from the steric effect within the confined space. On the other hand, the type of H-donor substrate is also an important factor for promoting the formation of $\mathbf{QH_2}$. The conversions of **Q** within the adsorption saturated **Q**/H_2O⊂CdL_2, **Q**/isopropanol⊂CdL_2 and **Q**/MeOH⊂CdL_2 are 13.0, 12.3 and 32.4% (Figure S11, ESI†), respectively. Compared to EtOH, the packing structure of these H-donors and **Q** within the CdL_2 pores might not facilitate the H-abstraction, consequently the solid-state photolysis.

Moreover, Cd(II)-MOF can also be a separator to effectively separate **Q** and $\mathbf{QH_2}$. As we know, **Q** and $\mathbf{QH_2}$ have the similar shape/size and often coexist together in some processes, so the separation of **Q** from $\mathbf{QH_2}$ is a big challenge. When the crystals of **1** were immersed in an EtOH solution that consists of **Q** and $\mathbf{QH_2}$ (**Q**/$\mathbf{QH_2}$ = 1:1 and 1:2, respectively) at ambient temperature for 7 days in dark. The ^{1}H NMR spectrum on the resulted crystals shows that **Q** is the preferred guest for the CdL_2 host in both cases. The selectivity of **1** is further supported by the liquid chromatographic (LC) measurement. The above **Q**/$\mathbf{QH_2}$ loaded crystals were extracted by MeOH, and the MeOH-extractions were used for the LC analysis. As shown in Figure 7, chromatographic measurement on the MeOH extracts of CdL_2 immersed in a EtOH solution of **Q**/$\mathbf{QH_2}$ (molar ratio, 1: 1 and 1 : 2) indicated that the the ratios of **Q**/$\mathbf{QH_2}$ are 4.6 : 1 and 3.2 : 1, respectively. So the porous CdL_2 framework can effectively separate **Q** and $\mathbf{QH_2}$ under ambient conditions.

In conclusion, we have reported **Q** adsorption/separation, sensing, and photoinduced transformation based on a porous Cd(II)-MOF framework in a SC-SC fashion. Notabtly, **Q** exists in the pores as a radical species in solar light, which makes the CdL_2 framework become a very sensitive luminescent sensor for probing **Q** under ambient conditions. Furthermore, the porous CdL_2 framework can be a specific molecular flask to successively upload different substrates, moreover, facilicates the sunlight induced **Q** transformation in the solid state. These results are in sharp contrast to those of common molecular adsorption and

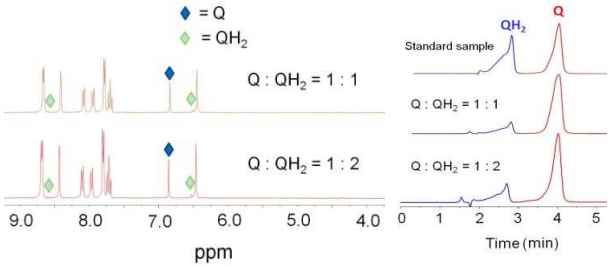

Figure 7. Left: ^{1}H NMR spectra (DMSO-d^6) recorded on the samples which were obtained by immersing of **1** in the EtOH solutions of **Q/QH$_2$** with the molar ratios at 1 : 1 and 1 : 2, respectively. The proton peaks of the encapsulated **Q** and **QH$_2$** are marked. Right: LC measurement. The standard sample was prepared by mixing equimolar amounts of **Q** and **QH$_2$** in MeOH. The MeOH-extractions of **Q/QH$_2$**⊂CdL_2 obtained from the EtOH solution of **Q/QH$_2$** at molar ratios of 1 : 1 and 1 : 2, respectively.

sensing behaviors based on MOFs, and reported photoinduced chemical transformations in aqueous and organic media.

We are grateful for financial support from NSFC (Grant Nos. 21271120, 21475078 and 21101100), 973 Program (Grant Nos. 2012CB821705 and 2013CB933800) and the Taishan scholar's construction project.

Notes and references

College of Chemistry, Chemical Engineering and Materials Science, Collaborative Innovation Center of Functionalized Probes for Chemical Imaging in Universities of Shandong, Key Laboratory of Molecular and Nano Probes, Ministry of Education, Shandong Normal University, Jinan 250014, P. R. China; E-mail: yubindong@sdnu.edu.cn

† Electronic Supplementary Information (ESI) available: Tables and figures for TGA, ^{1}H NMR spectra, XRPD patterns, chromatographic measurement, CIF file, crystal data. See DOI: 10.1039/b000000x/

‡ Synthesis of **2**. Compound **1** was sealed in a small vial full of **Q** vapour at 70°C for 48 h in dark to generate **2** (**[$CdL_2(ClO_4)_2$]•$C_6H_4O_2$**). IR(KBr pellet cm^{-1}): 3348(w), 1650(ms), 1604(s), 1523(ms), 1480(ms), 1402(ms), 1071(vs), 1010(ms), 881(ms), 795(s), 689(ms), 619(s). ^{1}HNMR (300MHz, DMSO, 25°C, TMS, ppm): 8.69-8.70 (d, J = 3.0Hz, 4H -C_5H_4N), 8.45 (s, 2H, -C_6H_4), 8.11-8.13 (d, J = 6.0Hz, 2H, -C_6H_4), 7.96-7.99 (d, J = 9.0Hz, 2H, -C_6H_4), 7.81-7.82 (d, J = 3.0Hz, 4H, -C_5H_4N), 7.70-7.75 (t, J = 15.0Hz, 2H, -C_6H_4), 6.86 (s, 1.6H, -C_6H_4O), 6.55 (s, 0.1H, -C_6H_6O), 6.45 (s, 2H, -NH_2). Elemental Analysis(%): calcd for $C_{54}H_{40}CdCl_2N_{12}O_{10}$: C 54.04, H 3.36, N 14.00; Found: C 54.17, H 3.28, N 14.05. Synthesis of **3**. Compound **2** was immersed in EtOH vapour for 2 days in dark to generate **3** (**[$CdL_2(ClO_4)_2$]•($C_6H_4O_2$)•(C_2H_5OH)]**). IR(KBr pellet cm^{-1}): 3348(w), 3069(w), 1651(ms), 1604(s), 1521ms), 1480(ms), 1402(ms), 1085(vs), 1008(ms), 881(ms), 796(s), 689(ms), 619(s). ^{1}HNMR (300MHz, DMSO, 25°C, TMS, ppm): 8.69-8.70 (d, J = 3.0Hz, 4H -C_5H_4N), 8.45 (s, 2H, -C_6H_4), 8.11-8.13 (d, J = 6.0Hz, 2H, -C_6H_4), 7.96-7.99 (d, J = 9.0Hz, 2H, -C_6H_4), 7.81-7.82 (d, J = 3.0Hz, 4H, -C_5H_4N), 7.70-7.75 (t, J = 15.0Hz, 2H, -C_6H_4), 6.87 (s, 1.6H, -C_6H_4O), 6.55 (s, 0.1H, -C_6H_6O), 6.47 (s, 2H, -NH_2), 4.32-4.35 (t, J = 9.0Hz, 0.6H, -OH), 3.41-3.48 (m, J = 21.0Hz, 1.3H, -CH_2-), 1.02-1.07 (t, J = 15.0Hz, 1.9H, -CH_3). Elemental Analysis(%): calcd for $C_{56}H_{46}CdCl_2N_{12}O_{11}$: C 53.97, H 3.72, N 13.49; Found: C 54.15, H 3.57, N 13.53. Synthesis of **4** (**[$CdL_2(ClO_4)_2$]•0.4($C_6H_4O_2$)•0.6($C_6H_6O_2$)**). Compound **3** was exposed to simulated solar light for 24h to generate **4**. IR (KBr pellet cm^{-1}): 3348(w), 3071(w), 1652(w), 1605(s), 1521ms), 1480(ms), 1402(ms), 1085(vs), 1008(ms), 882(ms), 796(s), 689(ms), 620(s). ^{1}H NMR (300MHz, DMSO, 25°C, TMS, ppm): 8.69-8.70 (d, J = 3.0Hz, 4H -C_5H_4N), 8.69 (s, 0.5H, -OH), 8.45 (s, 2H, -C_6H_4), 8.11-8.13 (d, J = 6.0Hz, 2H, -C_6H_4), 7.96-7.99 (d, J = 9.0Hz, 2H, -C_6H_4), 7.81-7.82 (d, J = 3.0Hz, 4H, -C_5H_4N), 7.70-7.75 (t, J = 15.0Hz, 2H, -C_6H_4), 6.86 (s, 0.6H, -C_6H_4O), 6.54 (s, 1.0H, -C_6H_6O), 6.46 (s, 2H, -NH_2), 4.32-4.35 (t, J = 9.0Hz, 0.17H, -OH), 3.41-3.48 (m, J = 21.0Hz, 0.25H, -CH_2-), 1.02-1.07 (t, J = 15.0Hz, 0.5H, -CH_3). Elemental Analysis(%): calcd for $C_{54}H_{41.2}CdCl_2N_{12}O_{10}$: C 53.98, H 3.46, N 13.99; Found: C 53.73, H 3.57, N 13.86.

Crystal data of **2**: Mr = 1200.28, *Tetragonal*, $P4_32_12$, a =15.8664(4), b = 15.8664(4), c = 21.7986(13) Å, V = 5487.7(4) Å^3, Z = 4, ρ = 1.453 gcm^{-3}, μ = 0.564 mm^{-1}, F(000) = 2440, GOF = 1.079; a total of 16438 reflections were collected in the range of 3.02° ≤ θ ≤ 25.60°, 4658 of which were unique (R_{int} = 0.0401); $R_1(wR_2)$ = 0.0433 (0.1109) for 421 parameters and 5167 reflections (I >2σ(I)). **3**: Mr = 1246.35, *Tetragonal*, $P4_32_12$, a =15.89830(10), b = 15.89830(10), c = 21.6675(7) Å, V = 5476.59(18) Å^3, Z = 4, ρ = 1.512 gcm^{-3}, μ = 0.570 mm^{-1}, F(000) = 2544, GOF = 1.071; a total of 16691 reflections were collected in the range of 3.02° ≤ θ ≤ 25.60°, 4594 of which were unique (R_{int} = 0.0412); $R_1(wR_2)$ = 0.0417 (0.0998) for 465 parameters and 5128 reflections (I >2σ(I)). **4**: Mr = 1201.50, *Tetragonal*, $P4_12_12$, a =15.90821(18), b = 15.90821(18), c = 21.6184(4) Å, V = 5471.00(13) Å^3, Z = 4, ρ = 1.458 gcm^{-3}, μ = 0.566 mm^{-1}, F(000) = 2444, GOF = 1.074; a total of 15884 reflections were collected in the range of 3.02° ≤ θ ≤ 25.60°, 4709 of which were unique (R_{int} = 0.0359); $R_1(wR_2)$ = 0.0417 (0.0998) for 465 parameters and 5142 reflections (I >2σ(I)). CCDC 1041609-1041611 contain the supplementary crystallographic data for this paper. These data can be obtained free of charge from The Cambridge Crystallographic Data Centre via www.ccdc.cam.ac.uk/data_request/cif.

1 H.-C. Zhou, J. R. Long, O. M. Yaghi, *Chem. Rev.* 2012, **112**, 673-674.

2 a) L. E. Kreno, K. Leong, O. K. Farha, M. Allendorf, R. P. V. Duyne, J. T. Hupp, *Chem. Rev.* 2012, **112**, 1105-1125. b) J.-R. Li, J. Sculley, H.-C. Zhou, *Chem. Rev.* 2012, **112**, 869-932. c) Y. Cui, Y. Yue, G. Qian, B. Chen, *Chem. Rev.* 2012, **112**, 1126-1162. d) H. Wu, Q. Gong, D. H. Olson, J. Li, *Chem. Rev.* 2012, **112**, 836-868.

3 J. Rebek Jr., *Acc. Chem. Res.* **2009**, *42*, 1660-1668.

4 a) D. Bradshaw, J. E. Warren, M. J. Rosseinsky, *Science* 2007, **315**, 977-980. b) O. Ohmori, M. Kawano, M. Fujita, *J. Am. Chem. Soc.* 2004, **126**, 16292-16293. c) M. C. Das, P. K. Bharadwaj. *J. Am. Chem. Soc.* 2009, **131**, 10942-10949. d) J. Tian, L. V. Saraf, B. Schwenzer, S. M. Taylor, E. K. Brechin, J. Liu, S. J. Dalgamo, P. K. Thallapally, *J. Am. Chem. Soc.* 2012, **134**, 9581-9584. e) H. Aggarwal, P. M. Bhatt, C. X. Bezuidenhout, L. J. Barbour, *J. Am. Chem. Soc.* 2014, **136**, 3776-3779. f) L. Ma, C.-D. Wu, M. M. Wanderley, W. Lin, *Angew. Chem. Int. Ed.* 2010, **49**, 8244-8248. g) Y.-G. Huang, B. Mu, P. M. Schoenecker, C. G. Carson, J. R. Karra, Y. Cai, K. S. Walton, *Angew. Chem. Int. Ed.* 2011, **50**, 426-440. h) J.-P Liang, Q.-F Xu, Z.-N Chen, B. F. Abrahams, *J. Am. Chem. Soc.* 2003, **125**, 12682-12683. i) D. Liu, J.-P Liang, B. F. Abrahams, *J. Am. Chem. Soc.* 2011, **133**, 11042-11045. j) Z. Niu, J.-G Ma, S. Wei, P. Cheng, *Chem. Commun.* 2014, **50**, 1839-1841. k) Z. Niu, S. Fang, J.-G Ma, X.-P Zhang, P. Cheng, *Chem. Commun.* 2014, **50**, 7797-7799.

5 a) M. Sittig, *Handbook of Toxic and Hazardous Chemicals and Carcinogens*. 2nd ed. Noyes Publications, Park Ridge, NJ. **1985**. b) W. Mbiya, I. Chipinda, P. D. Siegel, M. Mhike, R. H. Simoyi, *Chem. Res. Toxicol.* 2013, **26**, 112-123.

6 D. W. Roberts, A. O. Aptula, *Contact Dermatitis* **2009**, *61*, 332-336.

7 Z. Wu, M. Zhou, *Environ. Sci. Technol*. 2001, **35**, 2698-2703.

8 M. W. Anders, *Bioactivation of foreign compounds*, Academic Press, Inc.: New York, 1985, p 259.

9 a) Q.-K. Liu, J.-P. Ma, Y.-B. Dong, *Chem. Eur. J.* 2009, **15**, 10364-10368. b) Q.-K. Liu, J.-P. Ma, Y.-B. Dong, *J. Am. Chem. Soc.* 2010, **132**, 7005-7017.

10 Y. Aoyama, M. Asakawa, Y. Matsui, H. Ogoshi, *J. Am. Chem. Soc.* 1991, **113**, 6233-6240.

11 R. Chatterjee, C. S. Coates, S. Milikisiyants, O. G. Poluektov, K. V. Lakshmi, *J. Phys. Chem. B* 2012, **116**, 676-682.

12 A. M. Brouwer, C. Frochot, F. G. Gatti, D. A. Leigh, L. Mottier, F. Paolucci, S. Roffia, G. W. H. Wurpel, *Science* 2001, **291**, 2124-2128.

13 a) P. A. Leighton, G. S. Forbes, *J. Am. Chem. Soc.* 1929, **51**, 3549-3561. b) C. A. Bishop, K. J. Tong, *J. Am. Chem. Soc.* 1965, **87**, 501-505. c) H. M. Vyas, S. K. Wong, B. B. Adeleke, J. K. S. Wan, *J. Am. Chem. Soc.* 1975, **97**, 1385-1387. d) A. I. Ononye, J. R. Bolton, *J. Phys. Chem.* 1986, **90**, 6270-6274. e) J. von Sonntag, E. Mvula, K. Hildenbrand, C. von Sonntag, *Chem. Eur. J.* 2004, **10**, 440-451. f) K. Ohkubo, A. Fujimoto, S. Fukuzumi, *J. Am. Chem. Soc.* 2013, **135**, 5368-5371.

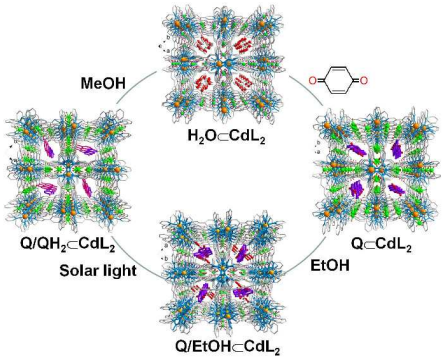

p-Benzoquinone (Q) adsorption/separation, sensing and its photoinduced transformation within a robust Cd(II)-MOF (**1**) is reported.